Int. J. Heat Mass Transfer. Vol. 13, pp. 1425–1439. Pergamon Press 1970. Printed in Great Britain

THE PEAK POOL BOILING HEAT FLUX ON HORIZONTAL CYLINDERS*

KAUO-HWA SUN† and JOHN H. LIENHARD‡
Dept. of Mech. Engineering, University of Kentucky, Lexington, Kentucky, U.S.A.

(*Received* 17 *July* 1969 *and in revised from* 15 *December* 1969)

Abstract—About 440 original observations of the peak pool boiling heat flux are presented for a wide range of sizes, gravities, reduced pressures and boiled liquids. These and an equal number of data for other conditions from the literature are correlated within about ±20 per cent accuracy on dimensionless heat flux versus dimensionless radius, coordinates.

An analytical prediction of the peak heat flux is developed. The prediction depends in part on a "vapor blanket thickness". Additional data provide the basis for an empirical expression for the blanket thickness. Substitution of this result in the analytical equation yields an accurate general equation for the peak heat flux.

NOMENCLATURE

A_g, area of the vapor jet, $\pi(R + \delta)^2$;
A_H, area of the heater surface per wavelength, $2\pi R\lambda_d$;
$f(\ )$, any undetermined function of( );
g, acceleration of a system in a force field;
g_e, earth normal gravity;
h_{fg}, latent heat of vaporization;
I, induced convection parameter, $\sqrt{(\rho_f \sigma L/\mu_f^2)}$;
M, molecular weight;
N, induced convection buoyancy parameter, I^2/R';
P, the parachor, $M\sigma^{\frac{1}{4}}/(\rho_f - \rho_g)$;
p_r, the reduced pressure, system pressure divided by the critical pressure, p_c;
q, q_{max}, q_{min}, heat flux; subscripts max and min denote the peak and minimum boiling heat fluxes, respectively;
q_{max_F}, q_{min_F}, Zuber's predicted peak and minimum heat fluxes for a flat plate;
R, characteristic length, equal to radius of a cylindrical heater in the present study;
$\mathscr{R}$, ideal gas constant;
R', dimensionless radius, $R[g(\rho_f - \rho_g)/\sigma]^{\frac{1}{2}}$;
T_c, critical temperature;
U_f, velocity of the liquid in the vicinity of the vapor jets;
U_g, U_{gc}, velocity of vapor jets. U_{gc} is critical value of U_g.

Greek letters

α, $g^{\frac{1}{4}}p_c(P/M)(8Mp_c/3RT_c)^{\frac{1}{2}}$;
Δ, an R′ based on $R = \delta$;
δ, the vapor blanket thickness on the horizontal diametral plane;
θ_c, the contact angle among liquid, vapor and the heater surface;
λ_d, most susceptible unstable wavelength, $2\pi(\sqrt{3})[\sigma/g(\rho_f - \rho_g)]^{\frac{1}{2}}$;
μ_f, liquid viscosity;

* This work was supported by NASA grant NGR-18-001-035 under the cognizance of Lewis Research Center.

† Research Assistant, Mechanical Engineering Dept., University of Kentucky, Lexington (presently at University of California, Berkeley).
‡ Professor of Mechanical Engineering, University of Kentucky, Lexington.

ρ_f, ρ_g, saturated liquid and vapor densities, respectively;

σ, surface tension between a saturated liquid and its vapor.

INTRODUCTION

THIS study is a part of an ongoing attempt to develop general descriptions of the interacting effects of gravity, g, and heater size upon the peak and minimum pool boiling heat fluxes, q_{max} and q_{min}. This development has generally centered upon the exploitation of expressions of the form:

$$\frac{q_{max}\,(\text{or } q_{min})}{q_{max_F}(\text{or } q_{min_F})} = f(\text{one or more scale parameters}) \quad (1)$$

to characterize the extreme heat fluxes. The subscript, F, designates the infinite horizontal flat plate configuration.

In the past, equation (1) has been used successfully in various forms to correlate data (see e.g. [1, 2]). It has been rationalized with the help of dimensional analysis [3]; and one equation of this form has been derived explicitly for the minimum heat flux on a horizontal cylinder [1, 4]. This correlation method reveals that the influence of gravity enters both through the well-known dependence of the extreme heat fluxes on $g^{\frac{1}{4}}$ for flat plates that is suggested by Zuber's flat plate predictions [5, 6] and through scale parameters as well.

The present paper, based upon [7], provides an analytical development of equation (1) for the peak heat flux on a horizontal cylinder. It substantiates this result with a great deal of original data, and data from the literature. Another basic result of the investigation is that it shows this method of handling the extreme heat fluxes breaks down when the capillary forces are two orders of magnitude or more larger than the gravity forces. For such small scale or very low gravity systems, the whole problem of either predicting or correlating extreme heat flux data appears to be farther out of reach than was previously suspected.

FUNCTIONAL FORM OF THE q_{max} EQUATION

In [3] it was shown by dimensional analysis that

$$\frac{q_{max}}{q_{max_F}} = f[R', I, \sqrt{(1 + \rho_g/\rho_f)}, \theta_c] \quad (2)$$

except in that θ_c, the contact angle among liquid, vapor and the heater surface, was ignored. Its addition here is legitimate since it is, itself, an independent dimensionless group which might, under some circumstances, influence q_{max}. The remaining groups are:

A *dimensionless peak heat flux*, q_{max}/q_{max_F}. Zuber's [5] prediction for the peak heat flux on an infinite horizontal flat plate

$$q_{max_F} = 0{\cdot}131\,(\sqrt{\rho_g})\,h_{fg}\,[\sigma g(\rho_f - \rho_g)]^{\frac{1}{4}} \quad (3)$$

is the best estimate of q_{max_F} available and it satisfies the dimensional analysis that led to equation (1). Therefore, we shall use it in this group.

A *dimensionless radius*, R', which is numerically equal the square root of the Bond or Laplace number. It is defined as

$$R' = R\sqrt{\left[\frac{g(\rho_f - \rho_g)}{\sigma}\right]} \quad (4)$$

where ρ_f and ρ_g are the saturated liquid and vapor densities, σ is the surface tension between a liquid and its vapor, and R is a characteristic dimension—the heater radius, in this case. When buoyant forces are great in comparison with capillary forces, R' is great, and vice versa. The dimensionless radius will be our basic scale parameter in this study.

An *induced convection scale parameter*, I. This is a second scale parameter defined as

$$I \equiv \sqrt{(\rho_f R\sigma/\mu_f^2)}. \quad (5)$$

It is possible to combine I and R' so as to obtain Borishanski's [8] *induced convection buoyancy parameter*, N

$$N \equiv I^2/R' \quad (6)$$

which (like the Prandtl number) is a physical property instead of a scale parameter.

A *vapor density term*, $\sqrt{(1 + \rho_g/\rho_f)}$. This term contributes little at low pressures. Zuber's equation (3) actually includes a factor which depends upon this term and which we have omitted. In [5] he shows that it contributes no more than 10 per cent variation to $q_{\max_F}$ over the entire range of p_r. What the effect of this term would be in other geometries, we do not know, but it is probably negligible at all pressures except those approaching the critical pressure in any configuration.

PREDICTION OF THE $q_{\max}$ EQUATION

The prediction of $q_{\max}$ will depend upon the following assumptions:

(1) The contact angle, θ_c, will not influence $q_{\max}$ significantly.

(2) Convection induced by the drag of rising bubbles will not seriously affect $q_{\max}$, nor will any other influence of viscosity be important.

(3) The vapor density is so much less than the liquid density that no significant inflow velocity of liquid will be required to balance the outflow of vapor.

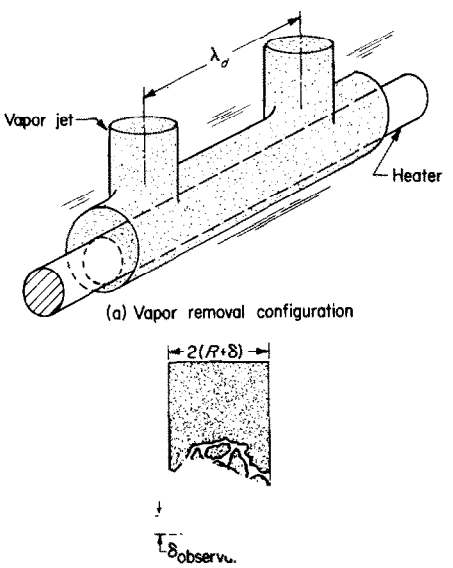

FIG. 1. Model for peak pool boiling heat flux on horizontal cylindrical heater, (R' on the order of unity).

These assumptions will have the effect of removing θ_c, I and $\sqrt{(1 + \rho_g/\rho_f)}$ from the problem and reducing equation (2) to

$$\frac{q_{\max}}{q_{\max_F}} = f(R'). \tag{7}$$

This is the functional form of the $q_{\max}$ expression that we are now seeking to derive.

The primary assumption that must be made is the idealization of the vapor removal configuration. Our vapor removal hypothesis is sketched in Fig. 1. We shall consider a horizontal cylindrical heater submerged in saturated liquid. Vapor is generated around the cylinder and rises in the direction of acceleration of the system. We imagine that there is a plane above the cylinder, where the bubbles from the upper half and lower half of the cylinder merge and form vapor columns. On this plane, the liquid is supported by the vapor in a Taylor-instable interface. The jets will be spaced on the Taylor-instable wavelength, λ_d, given by Bellman and Pennington [9] for a plane horizontal interface* as

$$\lambda_d = 2\pi(\sqrt{3})\sqrt{\left[\frac{\sigma}{g(\rho_f - \rho_g)}\right]}. \tag{8}$$

Instead of using Zuber's assumption that the radius of the vapor jets is $\lambda_d/4$, we shall assume that the jet radius is $(R + \delta)$ as indicated in Fig. 1. The wavelength on small wires could be as much as ten times the diameter, and it is implausible that the wire will produce a vapor jet with a diameter five times its own.

We have noted that the dimensionless radius is a scale parameter for the system, equal to the square root of the ratio of buoyancy to capillary

*This wavelength is chosen in preference to the wavelength derived by Lienhard and Wong [4] for a cylindrical interface. The latter wavelength was based upon an interface curvature which is not replicated in the present peak heat flux configuration.

forces in the system. When R' is very large, the unstable wavelength, λ_d, is much smaller than $2(R + \delta)$ and the scale effect should vanish. Therefore q_{max}/q_{max_F} should approach a constant limiting value in this case. When R' is on the order of unity, λ_d and $2(R + \delta)$ are comparable to each other and it is necessary to consider a fairly complex interaction of capillary and gravity effects. We shall accordingly undertake the prediction of q_{max} in two stages—one for R' on the order of unity and one for R' large. The problem of predicting q_{max} when $R' \ll 1$ will not be undertaken here.

The peak heat flux when R′ *is on the order of unity.* We shall base the analysis upon consideration of a "unit cell" of one wavelength, λ_d. If A_H is the area of the heater surface within a cell and A_g is the cross-sectional area of a vapor jet, then

$$\frac{A_g}{A_H} = \frac{\pi(R + \delta)^2}{2\pi R\lambda_d} = \frac{(R + \delta)^2}{2R\lambda_d}. \tag{9}$$

The heat flux, q, from the heater during saturated boiling is balanced by the latent heat carried away in the vapor bubbles. Since all the bubbles merge and form vapor jets with area, A_g, we can write an energy balance in the form

$$q = \rho_g h_{fg} U_g \frac{A_g}{A_H} = \rho_g h_{fg} U_g \frac{(R + \delta)^2}{2R\lambda_d} \tag{10}$$

where U_g is the velocity of the vapor in the jet. The heat flux reaches q_{max} when the velocity of the vapor jets reaches the critical value, U_{gc}, at which they become Helmholtz-instable. Therefore,

$$q_{max} = \rho_g h_{fg} U_{gc} \frac{(R + \delta)^2}{2R\lambda_d}. \tag{10a}$$

Next we must determine U_{gc}. We shall assume, as Zuber did, that the Helmholtz-instable collapse of the jet occurs as a result of a major disturbance arising from Rayleigh's capillary instability. According to Rayleigh ([10], p. 473), the minimum wavelength that will be capillary-instable is one circumference, or $2\pi(R + \delta)$, in length. This will be the major disturbance in the jet and will be Helmholtz-instable when U_g reaches a value U_{gc} such that ([10], p. 462)

$$2\pi(R + \delta) = 2\pi \frac{\rho_f + \rho_g}{\rho_f \rho_g} \left[\frac{\sigma}{(U_f + U_{gc})^2}\right]. \tag{11}$$

Thus, if we neglect the velocity, U_f, of liquid in-flow, and assume $\rho_g \ll \rho_f$,

$$U_{gc} = \sqrt{\left[\frac{\sigma}{\rho_g(R + \delta)}\right]}. \tag{12}$$

Substituting equation (12) into equation (10a) gives the equation for the peak heat flux on a horizontal cylinder

$$q_{max} = \frac{(R + \delta)^2}{2R\lambda_d} \rho_g h_{fg} \sqrt{\left[\frac{\sigma}{\rho_g(R + \delta)}\right]}. \tag{13}$$

While the radius of the cylinder and the physical properties are known, the vapor blanket thickness, δ, remains to be determined. If we define a dimensionless vapor blanket thickness

$$\Delta \equiv \delta[g(\rho_f - \rho_g)/\sigma]^{\frac{1}{2}} \tag{14}$$

and combine equations (8) and (14) with equation (13), we get

$$q_{max} = \left\{\frac{\pi}{24}(\sqrt{\rho_g})\, h_{fg}[\sigma g(\rho_f - \rho_g)]^{\frac{1}{4}}\right\} \left\{\frac{6}{\pi^2(\sqrt{3})} \frac{(R' + \Delta)^{\frac{3}{2}}}{R'}\right\}. \tag{15}$$

The first group on the right-hand side of equation (15) contains a constant which has been balanced against the second term so that it matches Zuber's flat plate prediction, q_{max_F}. Thus

$$\frac{q_{max}}{q_{max_F}} = \frac{6}{\pi^2(\sqrt{3})} \frac{(R' + \Delta)^{\frac{3}{2}}}{R'} \tag{16}$$

where Δ remains to be determined with the help of experiments.

Prediction of q_{max} *for large* R'. As R' increases, and capillary forces cease to exert an influence on q_{max}, the analytical model presented in the

previous section should yield to one that is independent of R'.

We have assumed that vapor jets with a radius of $(R + \delta)$ are spaced on the wavelength, λ_d. But λ_d and the spacing between jets will decrease as R' increases. According to the previous analytical model, the jets will touch one another when $(R' + \Delta)$ reaches $2\pi(\sqrt{3})/2$.

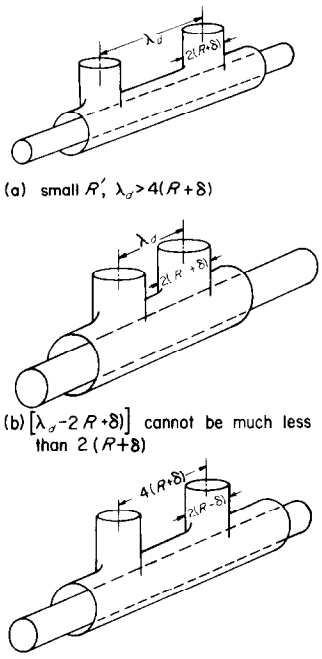

FIG. 2. Variation of jet spacing as R' changes.

However, we did not see this happen in the present investigation of pool boiling.* Therefore, the preceding model should fail at some $(R' + \Delta)$ smaller than $\pi\sqrt{3}$. An illustrative sequence of sketches showing the supposed variation of the jets with increasing R' is given in Fig. 2.

When R' is small, the unstable wavelength, λ_d, is greater than twice the jet diameter, $4(R + \delta)$, as shown in Fig. 2a. As R' increases, the difference between λ_d and $4(R + \delta)$ becomes smaller. We believe that, when R' is very large, the open space between two jets will be equal to $2(R + \delta)$ and the jet configuration will remain unchanged. The jets will stay as shown in Fig. 2c instead of moving any closer as indicated in Fig. 2b. This is analogous to Zuber's assumption that the jet diameter on a flat plate is equal to the open space between two jets, and our photographic studies verified that it is a realistic assumption.

When R' becomes very large, disturbances with the wavelength, λ_d, will exist in the horizontal vapor–liquid interface, but they will be much smaller than the jet diameter. The vapor jets will pick up these disturbances from the intervening liquid–vapor interface. It is probably this disturbance that triggers Helmholtz instability instead of the longer wavelength of the Rayleigh-instability. Thus we shall assume that the jet diameter is $2(R + \delta)$, but that the distance between centerlines of jets is $4(R + \delta)$ instead of λ_d. Finally, we use λ_d instead of $2\pi(R + \delta)$ for the left-hand side of equation (11) and obtain

$$U_{gc} = \sqrt{\left(\frac{2\pi\sigma}{\rho_g \lambda_d}\right)} \tag{17}$$

in the place of equation (12).

Combining equations (8) and (17) with equation (10a) gives

$$q_{\max} = \left[\frac{\pi}{24}\rho_g h_{fg} \sqrt[4]{\left(\frac{\sigma g(\rho_f - \rho_g)}{\rho_g^2}\right)}\right] \left[\frac{3^{\frac{1}{2}}}{\pi}\frac{(R' + \Delta)}{R'}\right] \tag{18}$$

or

$$\frac{q_{\max}}{q_{\max_F}} = \frac{3^{\frac{1}{2}}}{\pi}\frac{(R' + \Delta)}{R'}. \tag{19}$$

Equations (16) and (19) should each give the same peak heat flux at the point where one configuration shifts to another. Thus, we can write, for this particular value of R',

$$\frac{3^{\frac{1}{2}}}{\pi}\frac{(R' + \Delta)}{R'} = \frac{6}{\pi^2\sqrt{3}}\frac{(R' + \Delta)^{\frac{1}{2}}}{R'}. \tag{20}$$

* It was observed by Vliet and Leppert [11] that, in a strong forced convection boiling system, no jetting occurred. The vapor appeared instead to cover the whole wake region of the cylinder.

This gives, for the transition between the two analytical models,

$$R' + \Delta = 4{\cdot}28. \tag{21}$$

Finally, the expression for q_{max} at very large R' should become

$$\frac{q_{max}}{q_{max_F}} = \frac{3^{\frac{1}{2}}}{\pi}\frac{R' + \Delta}{R'} = \text{constant}, \qquad R' + \Delta \geqslant 4{\cdot}28 \tag{19a}$$

where the dimensionless vapor blanket thickness still must be determined. Once Δ is known at $(R' + \Delta) = 4{\cdot}28$, the constant in equation (19a) can be fixed.

The jet diameter reaches $\lambda_d/2$ at $(R' + \Delta) = \pi(\sqrt{3})/2$ according to the model for R' on the order of unity. Beyond this size the open space between the two jets must become less than the jet diameter (or, conversely, the jet spacing might start to increase beyond λ_d) until $(R' + \Delta)$ reaches 4·28. Thus $(R' + \Delta) = 4{\cdot}28$ is actually the upper bound for a transition which might occur gradually over the range $\pi(\sqrt{3})/2 < (R' + \Delta) < 4{\cdot}28$.

We now need to provide experimental verification of three kinds: Photographic evidence is required to verify our assumed removal configurations. It remains to be proven that the functional equation (2) really does reduce to equation (7), and this will require a great number of q_{max} data. And δ must be measured over a wide range of R' to eliminate Δ from equations (16) and (19). Then it will be possible to compare the theoretical expressions with the correlation to determine whether or not they are a success.

EXPERIMENT

Measurements of q_{max} on nichrome wires 4 in. in length, in 4 reagent-grade organic liquids (acetone, methanol, benzene and isopropanol) were made in the capsule shown in Fig. 3. The capsule is 3·5 in. wide, 3·5 in. high and 7 in. long with two $\frac{1}{4}$ in. thick plate glass windows in the 3·5 by 7 walls. A one-in. marker was mounted on the bottom of the capsule to provide a reference dimension for the reduction of photographic data. A low thermal capacity ceramic-coated resistance heater was mounted close to the bottom of the test section as a preheater. Styrofoam, $\frac{1}{4}$ in. thick, was glued around the test capsule to minimize the heat losses during the experiments.

Nichrome wire heating elements, ranging in

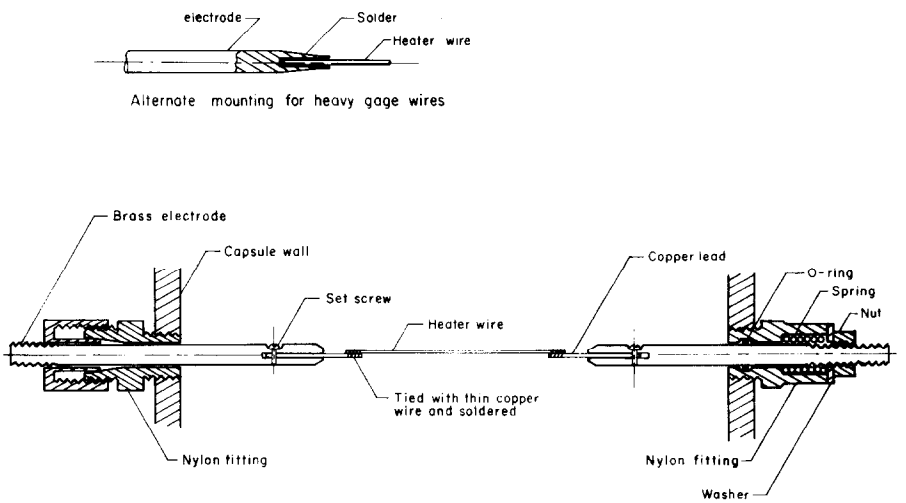

FIG. 4. Configuration of cylindrical heater wire attachment.

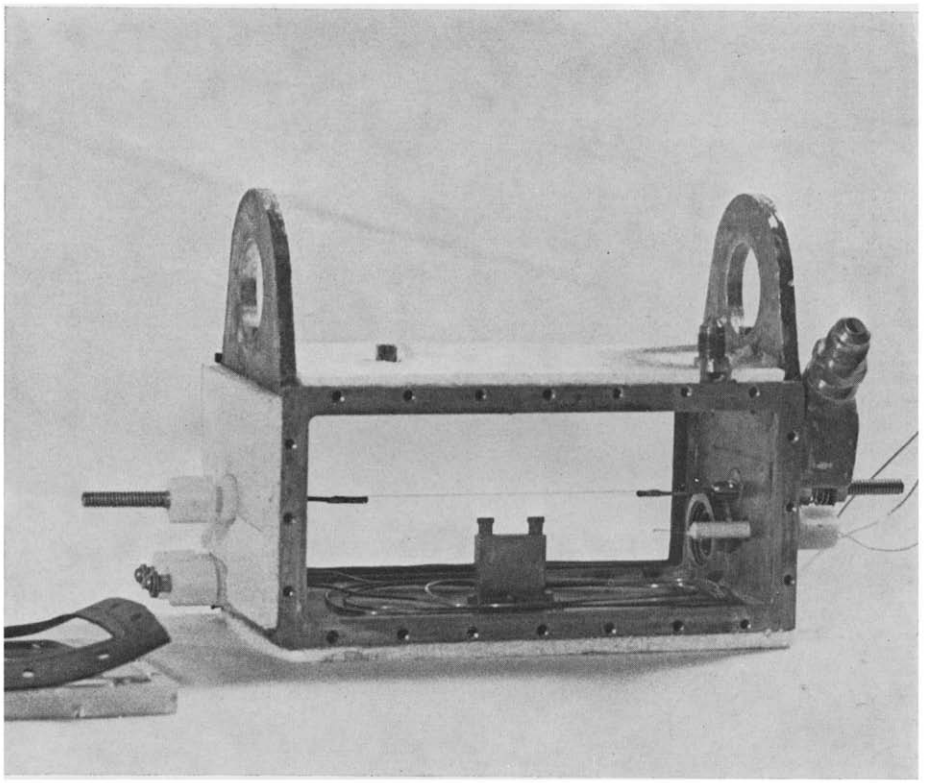

FIG. 3. A test capsule.

[*facing page* 1430]

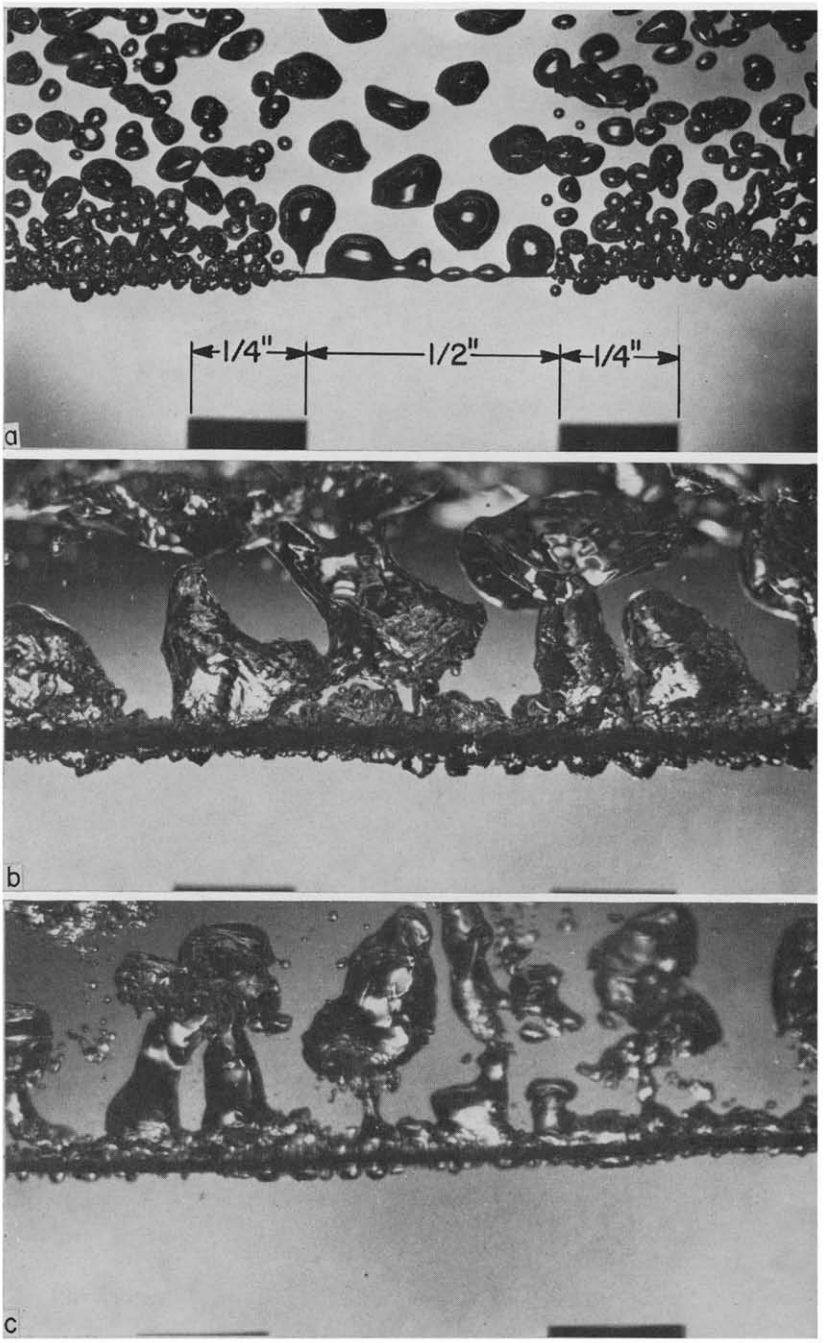

FIG 6. Photographs of nucleate boiling at q just below q_{max}.

(a) $g/g_e=1$, $R=0{\cdot}0040$ in., methanol, $q=158\,000$ Btu/ft²h, $R'=0{\cdot}0645$.
(b) $g/g_e=1$, $R=0{\cdot}0255$ in., benzene, $q=110\,200$ Btu/ft²h, $R'=0{\cdot}388$.
(c) $g/g_e=9{\cdot}9$, $R=0{\cdot}0127$ in., methanol, $q=330\,000$ Btu/ft²h, $R'=0{\cdot}642$.

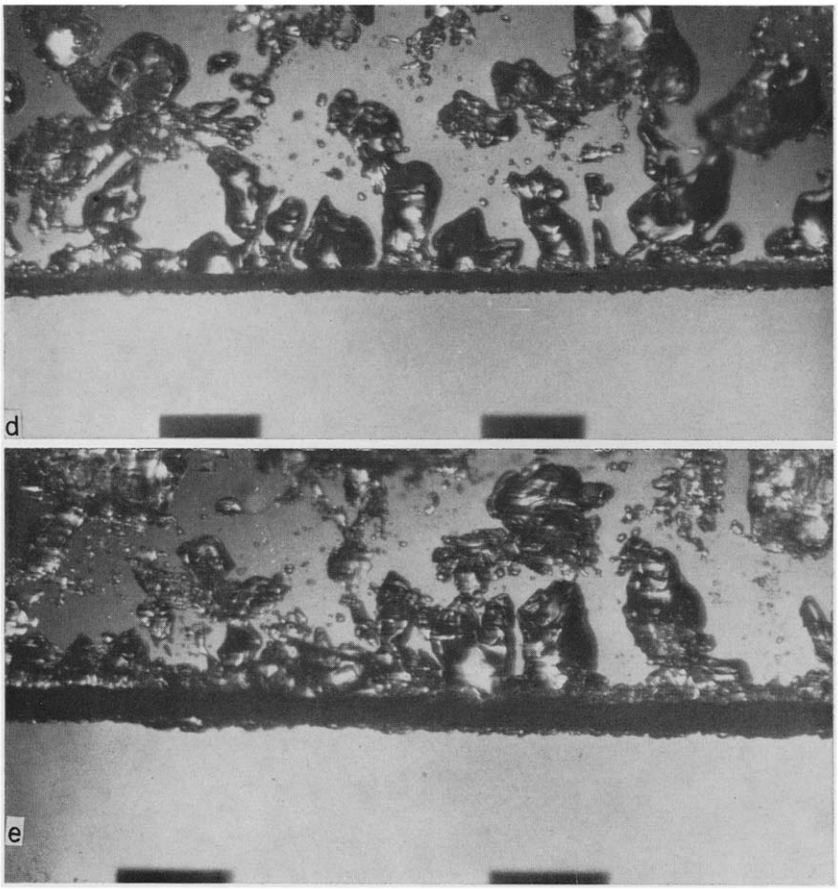

FIG. 6. *continued.*

(d) $g/g_e=14{\cdot}7$, $R=0{\cdot}0200$ in., isopropanol, $q=235\,000$ Btu/ft²h, $R'=1{\cdot}281$.
(e) $g/g_e=26{\cdot}8$, $R=0{\cdot}0320$ in., methanol, $q=311\,000$ Btu/ft²h, $R'=2{\cdot}68$.

size from 0·0050 to 0·0810 in. dia., were mounted as shown in Figs. 3 and 4. For wire sizes larger than gage 16, the wires were soldered directly to a tapered brass lead, as shown in Fig. 4. All wires were at least 6 times longer than the "unit cell".

A centrifuge shown in Fig. 5 was designed and built to operate at speeds up to 360 rpm, which corresponds with a gravity of about 100 times earth normal gravity. The centrifuge facility is described in detail, in [12].

Before each test the wires were cleaned with soap and hot water, and then rinsed with acetone.

The preheater was used to bring the liquid to its saturation temperature and maintain it there for at least 10 min. It was then turned off to get rid of both bubbles and convective currents, and to avoid any effects of electric fields. The current in the nichrome heater was then increased steadily until the transition from nucleate to film boiling was observed: The voltage or

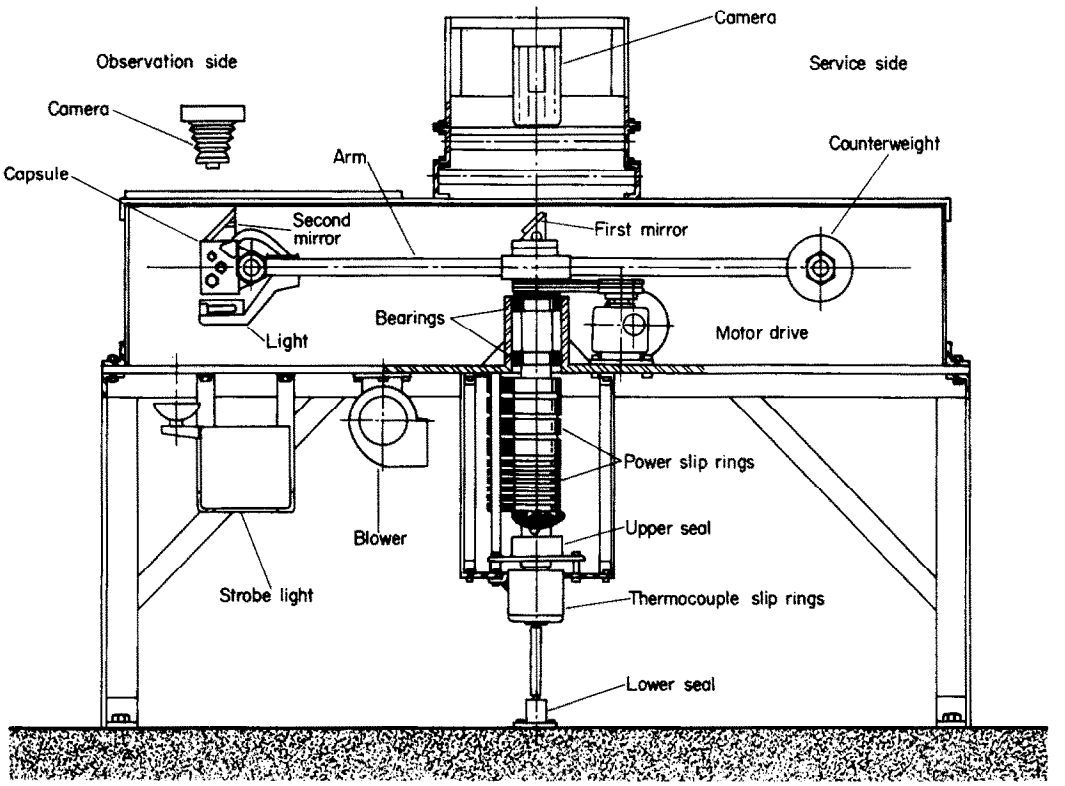

FIG. 5. Cross-sectional view of complete centrifuge apparatus.

A strobe light beneath the path of the test capsule was triggered by a photoelectric pick-off by each revolution. Thus, the test capsule appeared stationary to the eye and the boiling phenomenon could either be observed or photographed. A Hycam high-speed motion picture camera was also used to take continuous motion pictures.

current was then recorded. The same process was repeated several times to assure that the voltage or current was generally reproducible.

The peak heat fluxes were calculated from the measured voltage or current, the resistance of the wire, and the measured heater dimensions. The resistance was determined from voltage or current measurements made in the nucleate

boiling regime close to the transition point immediately after each set of observations. For different runs, the wires and liquid were replaced by new ones to avoid effects of contamination of the liquid or of carbon deposits on the wire surface. If the transition started consistently from the end of the wire, which might indicate serious end effects, the wire was not used. An error analysis showed that the probable error in our reduced q_{max} observation was $\pm 4{\cdot}1$ per cent.

During both stationary and centrifuge tests, about 640 pictures and several high speed motion pictures were taken at arbitrary heat fluxes very close to the transition point. They cover the range of R' from 0·0645 up to 4·375. Five of these photographs are included in Fig. 6.

About 440 q_{max} data were recorded over the range of heater sizes and gravities—170 in acetone, 77 in benzene, 85 in isopropanol and 106 in methanol. These data are tabulated in [7]. The probable errors of the dimensionless variables, q_{max}/q_{max_F} and R' were about $\pm 4{\cdot}4$ per cent and $\pm 2{\cdot}9$ per cent, respectively.

PRESENTATION AND DISCUSSION OF RESULTS

Correlation of q_{max} *data.* A total of about 900 q_{max} data were collected in this study. They were obtained both from the present experiments and from other sources. The observed q_{max} were divided by Zuber's q_{max_F}, which was computed with some care in [7] and is plotted for typical fluids in Fig. 7.

Figure 8 displays the present data, as well as data of Cumo *et al.* [13] and Lienhard and Watanabe [1], in the range $R' < 0{\cdot}5$. It includes data for acetone, benzene, carbon tetrachloride, isopropanol, methanol and water over wide ranges of pressure, gravity and heater size. The variability of the data is on the order of ± 20 per cent except when $R' < 0{\cdot}15$.

The correlation curve from [1] has also been included. This curve was originally presented on (q_{max}/α) vs. R' coordinates, where α is a function of thermodynamic constants for the liquid, derived with the aid of the Law of Corresponding States in [14]. The values of (q_{max}/α) in [14] were multiplied by (α/q_{max_F}) for acetone to place it in the present coordinates. The small irregularities in this correlation are probably related to changes of the transition mechanism, too small to be accounted in our relatively coarse analysis.

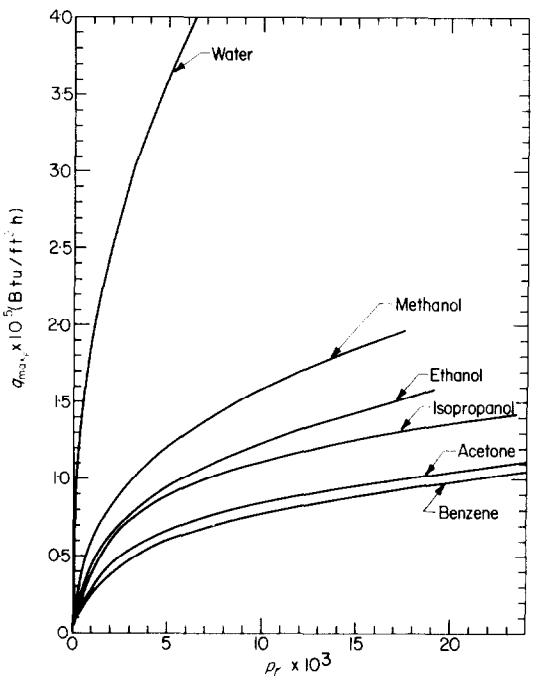

FIG. 7. Zuber's q_{max_F} prediction for flat plate heaters

Figure 9 shows our data for a larger range of R'. Data given by Adams [15], Carne [16], Costello and Heath [17], Cumo *et al.* [13], Frea and Costello [18] and Pramuk and Westwater [19] are also included. All these data correlate consistently in q_{max}/q_{max_F} vs. R' coordinates.

Figure 10 shows our data for high R' and additional data from [15] and [17]. The data appear to approach a constant value of q_{max}/q_{max_F} for large R' as we anticipated. This tendency was also observed by Lienhard and Keeling [3] in their study of horizontal ribbon heaters. Lyon's [20] data for boiling liquid N_2 and O_2

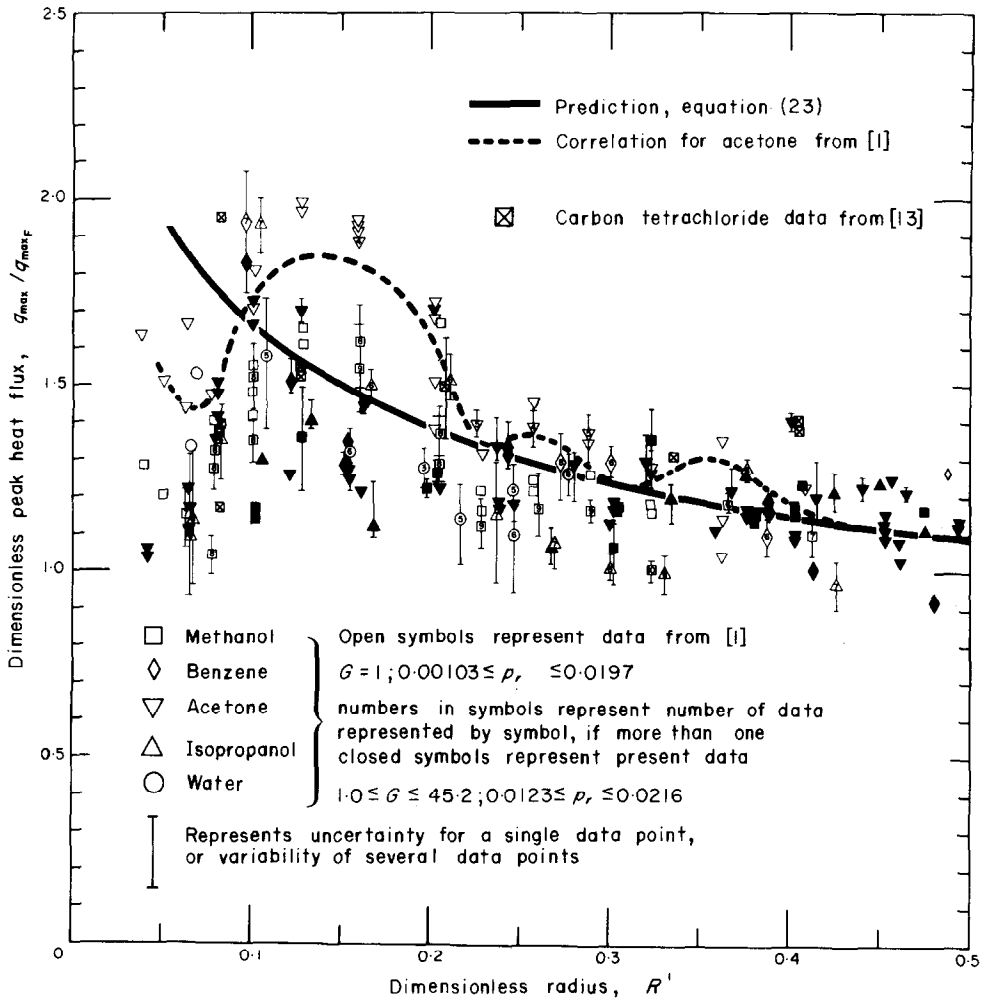

FIG. 8. Comparison of prediction with experimental data for $R' < 0{\cdot}50$.

are also included in Fig. 10. They all fall within the scatter of ± 20 per cent.

Figure 11 is a general view of the results of the correlation. A variety of very low R' data obtained by Siegel and Howell [21] under reduced-gravity conditions are also included. The correlation is shown to be very successful with the existing data for all $R' > 0{\cdot}15$, but when $R' < 0{\cdot}15$, the data show a wide scatter.

The success of equation (7) in bringing together so many diverse data indicates that the three assumptions upon which it is based must be correct. In particular, it is most heartening to discover that surface condition has not proved to be important—at least for $R' > 0{\cdot}15$. Some further commentary on this is in order:

Cichelli and Bonilla [22] first indicated that q_{max} was 15 per cent higher for "dirty" surfaces than for "clean" surfaces. Berenson [23] subsequently showed that while q_{max} data for flat plate heaters were insensitive to surface roughness, they could be altered slightly by θ_c. This is

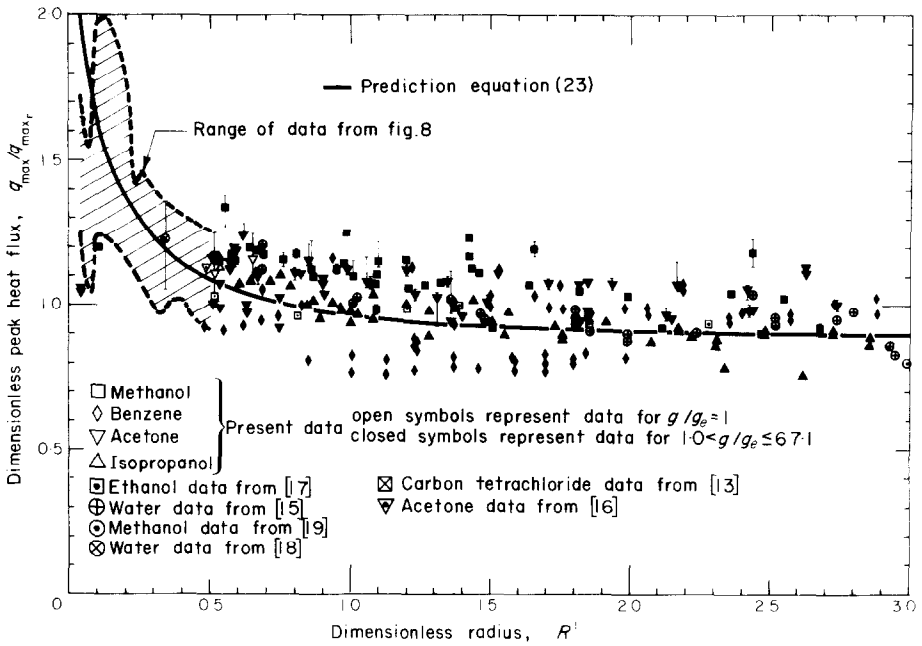

FIG. 9. Comparison of prediction with experimental data for $R' < 3{\cdot}0$.

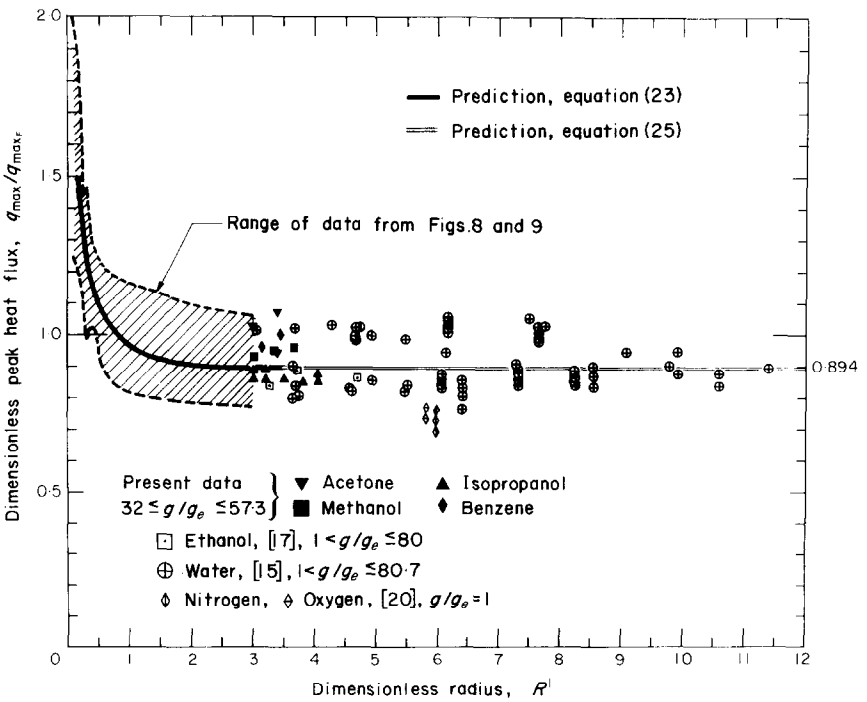

FIG. 10. Comparison of prediction with experimental data for very large R'.

because the peak heat flux transition is primarily governed by a hydrodynamic stability away from the heater, and only indirectly related to action at the heater surface. Lyon also showed that his q_{max} data for liquid N_2 and O_2 were independent of the surface roughness, but that severe changes in the chemical and thermal nature of the surface could alter q_{max} by 25 per cent or more.

In the present study, we have collected data for many smooth and very clean surfaces, in which only θ_c might have been subject to variation. Only in the very low R' range de we discover a failure of the simple correlation scheme. This might imply either technical difficulties in obtaining the experimental data or that equation (7) is incomplete in the low R' range. In particular θ_c or I might be important independent variables. The photographic studies (see e.g. Fig. 6a) showed that bubble growth and

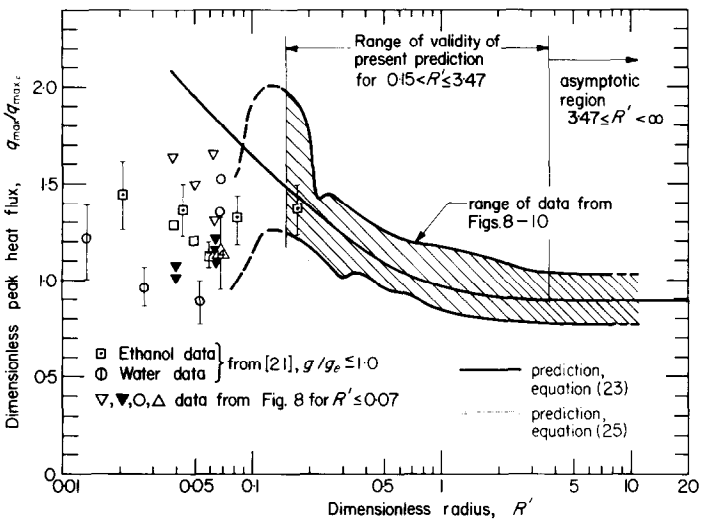

FIG. 11. General view of the results of the present correlation.

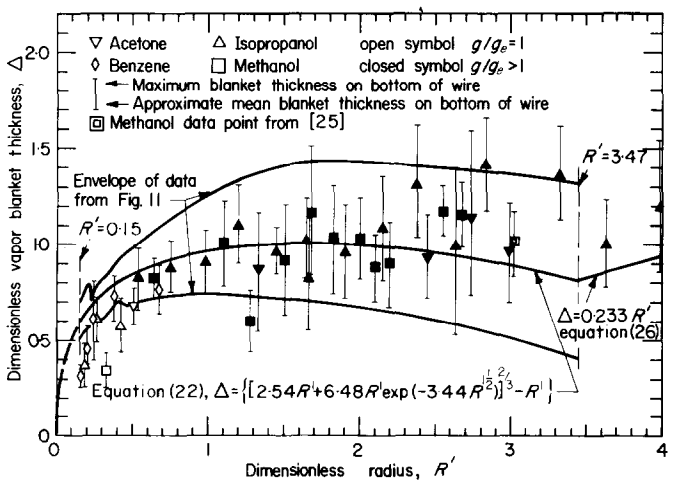

FIG. 12. Experimental determination of the vapor blanket thickness.

merger mechanisms govern the vapor removal process at very small R'. In this range, both viscosity and contact angle may become very significant.

Results of the photographic studies. Our analytical model for the transition mechanism was based upon considerable study of motion pictures and still photographs such as are shown in Fig. 6. These showed that as R' dropped from 0·15 down to 0·07 the jets gradually vanished. Instead, small bubbles grew on the surface and merged into larger ones until, at a high enough heat flux, the bubble population became so crowded that transition occurred. The deterioration of a Taylor-instability dominated transition into a bubble merger transition was also observed at $R' \simeq 0{\cdot}07$ in. film boiling by Lienhard and Sun [24]. Serious bubble-merging is shown at $R' = 0{\cdot}0645$ in Fig. 6a, in which transition has already occurred at the center and is progressing toward the ends.

The subsequent figures show the existence of the merging plane. They indicate that vapor jets do not originate from the heater surface, but develop somewhere above the heater where the bubbles from both the lower and upper halves of the heater surface merge. They also show clearly that the vapor escape route is through vapor jets.

The vapor blanket thickness data required to complete equations (16) and (19) was also obtained from the photographic study. Since we view the vapor blanket from the side, δ cannot be measured on the horizontal diametral plane. Hence, we had to approximate δ with a measurement of the blanket thickness on the bottom part of the cylinder as shown in Fig. 1b.

Figure 12 displays the measurements of δ. In an attempt to compensate the fact that the blanket is not fully developed at the bottom, we have reported the range from the approximate mean, to the maximum size of the bubbles comprising the blanket. A data point measured from an early photograph by Westwater and Santangelo [25] is also included. The uncertainty of these measurements is on the order of ± 20 per cent. No attempt was made to measure δ in the range of $R' < 0{\cdot}15$.

If we combine the envelope of the data from Fig. 11 with equation (16), we can specify a range of Δ, consistent with the $q_{\max}$ theory, for each value of R'. The result is plotted in Fig. 12. Virtually all the measurements of δ fall within this envelope.

The "best fit" empirical equation, based on both this envelope and the data for δ, is

$$\Delta = [2{\cdot}54\,R' + 6{\cdot}48\,R' \exp(-3{\cdot}44\sqrt{R'})]^{\frac{1}{2}} - R' \qquad (22)$$

in the range: $0{\cdot}15 < R' < 3{\cdot}5$. The form of equation (22) is chosen so as to give a neat form for the $q_{\max}/q_{\max_F}$ equation that we shall develop next.

Completion of the q_{max} *predictions.* The substitution of equation (22) in equation (16) yields

$$\frac{q_{\max}}{q_{\max_F}} = 0{\cdot}89 + 2{\cdot}27\exp(-3{\cdot}44\sqrt{R'}). \qquad (23)$$

Equation (23) is plotted in Figs. 8–11 and it shows very good agreement with the existing data.

The upper limit of equation (23)—the transition point between the two models—is determined by equation (21). With the help of equation (22), we obtain

$$R' = 3{\cdot}47 \qquad \text{at} \qquad R' + \Delta = 4{\cdot}28. \qquad (24)$$

The constant value for $q_{\max}/q_{\max_F}$ in equation (19a) can now be fixed with the help of equations (24) and (22):

$$\frac{q_{\max}}{q_{\max_F}} = \frac{3^{\frac{1}{2}}}{\pi}\frac{4{\cdot}28}{3{\cdot}47} = 0{\cdot}894; \qquad R' > 3{\cdot}47. \qquad (25)$$

Thus the proper upper bound on equation (22) is $R' = 3{\cdot}47$, and the relation between Δ and R', for $R' > 3{\cdot}47$, can be found by combining (19a) with equation (25) to get

$$\Delta = 0{\cdot}233\,R' \qquad R' > 3{\cdot}47. \qquad (26)$$

Equation (26), plotted on Fig. 12, is consistent

with the few measured values of the vapor blanket thickness in this range.

Figure 13 shows equation (16) for various values of Δ and the semi-theoretical equation for q_{max}/q_{max_F}. Actually equation (23) differs negligibly from equation (25) for $R > 3{\cdot}47$. Therefore equation (23) can properly be used for the entire range of $R' > 0{\cdot}15$.

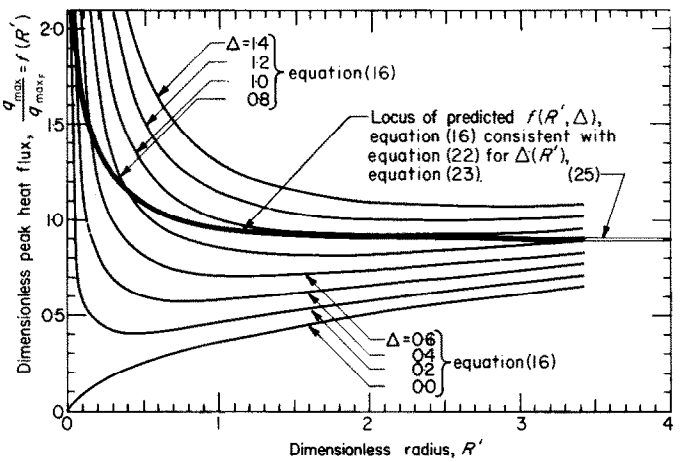

FIG. 13. Theoretical peak heat fluxes for various values of Δ, compared with final prediction.

We have presented two models for the q_{max} transition. Actually, there are small aspects of the transition mechanisms which are ignored in these relatively simple descriptions. The range of R' between 1·72, at which $(R' + \Delta) = \pi(\sqrt{3})/2$, and 3·47 is, for example, a transition range between two models. As R' increases in this range, the jet-spacing becomes decreasingly dependent on λ_d.

CONCLUSIONS

1. A hydrodynamic model is developed for the prediction of q_{max} on horizontal cylinders. The resulting expressions are

$$\frac{q_{max}}{q_{max_F}} = \frac{6}{\pi^2\sqrt{3}} \frac{(R' + \Delta)^{\frac{1}{2}}}{R'}; \quad R' + \Delta \leqslant 4{\cdot}28$$

and

$$\frac{q_{max}}{q_{max_F}} = \frac{3^{\frac{1}{2}}}{\pi} \frac{R' + \Delta}{R'} = \text{constant}; \quad R' + \Delta > 4{\cdot}28.$$

2. About 900 q_{max} data for cylindrical heaters of various sizes, under different pressure and gravity conditions, and in a variety of liquids were correlated successfully on q_{max}/q_{max_F} vs. R' coordinates.

3. The dimensionless vapor blanket thickness, Δ, is determined by an empirical equation

$$\Delta = [2{\cdot}54\,R' + 6{\cdot}48\,R' \exp(-3{\cdot}44\sqrt{R'})]^{\frac{1}{2}} - R'; \quad R' < 3{\cdot}47$$

from which we find that $R' = 3{\cdot}47$ at $R' + \Delta = 4{\cdot}28$. Therefore,

$$\Delta = 0{\cdot}233\,R' \quad R' > 3{\cdot}47.$$

4. The resulting equation for q_{max} on horizontal cylinders is

$$q_{max}/q_{maxF} \simeq 0{\cdot}890 + 2{\cdot}27 \exp(-3{\cdot}44\sqrt{R'}); \quad 0{\cdot}15 < R'.$$

5. When $R' < 0{\cdot}15$, the q_{max} data start deviating from the prediction and scatter widely on the q_{max}/q_{maxF} vs. R' coordinates. When $R' < 0{\cdot}07$, the peak heat flux transition is governed by another type of instability in which the gravity force is over-balanced by capillary forces.

REFERENCES

1. J. H. LIENHARD and K. WATANABE, On correlating the peak and minimum boiling heat fluxes with pressure and heater configuration, *J. Heat Transfer* **88**, 94 (1966).
2. J. H. LIENHARD, Interacting effects of geometry and gravity upon the extreme boiling heat flux, *J. Heat Transfer* **90**, 178 (1968).
3. J. H. LIENHARD and K. B. KEELING, An induced convection effect upon the peak heat flux, *J. Heat Transfer* **92**, 1 (1970).
4. J. H. LIENHARD and P. T. Y. WONG, The dominant unstable wavelength and minimum heat flux during film boiling on a horizontal cylinder, *J. Heat Transfer* **86**, 220 (1964).
5. N. ZUBER, M. TRIBUS and J. W. WESTWATER, The hydrodynamic crisis in pool boiling of saturated and subcooled liquids, *Int. Dev. in Heat Transfer*, pp. 230–235. ASME, New York (1963).
6. N. ZUBER, Hydrodynamic aspects of boiling heat transfer, Atomic Energy Commission Report No. AECU-4439, Physics and Mathematics, June 1959.
7. K. H. SUN, The peak pool boiling heat flux on horizontal cylinders, M.S. Thesis, University of Kentucky, 1969 (available as College of Engineering Bulletin No. 88, May 1969).
8. V. M. BORISHANSKI, An equation generalizing experimental data on the cessation of bubble boiling in a large volume of liquid, *Zh. Tekh. Fiz.* **25**, 252 (1956).
9. R. BELLMAN and R. H. PENNINGTON, Effects of surface tension and viscosity on Taylor instability, *Q. Appl. Math.* **12**, 151 (1954).
10. H. LAMB, *Hydrodynamics*, 6th ed. Dover, New York (1945).
11. G. C. VLIET and G. LEPPERT, Critical heat transfer for nearly saturated water flowing normal to a cylinder, *J. Heat Transfer* **86**, 59–67 (1964).
12. J. H. LIENHARD and W. M. CARTER, Gravity boiling studies, 1st annual report, Technical Report No. 1-68-ME-1, University of Kentucky (1968).
13. M. CUMO, G. E. FARELLO and G. C. PINCHERA, Some aspects of free convection boiling heat transfer, *Congresso A.T.I., Genova*, September 1965.
14. J. H. LIENHARD and V. E. SCHROCK, The effect of pressure, geometry and the equation of state upon the peak and minimum boiling heat flux, *J. Heat Transfer* **85**, 261 (1963).
15. J. M. ADAMS, A study of the critical heat flux in an accelerating pool boiling system, Ph.D. thesis, Mechanical Engineering Department, University of Washington, September 1962. (also released, as Heat Transfer Lab. report).
16. M. CARNE, Studies of the critical heat flux of some binary mixtures and their components, *Can. J. Chem. Engng* pp. 235–241, Dec. 1963.
17. C. P. COSTELLO and C. A. HEATH, The interaction of surface effects and acceleration in the burnout heat flux problem, *A.I.Ch.E.Jl* **10**, 278–288 (1964).
18. W. J. FREA and C. P. COSTELLO, Mechanisms for increasing the peak heat flux in boiling saturated water at atmospheric pressure, Report, Heat Trans. Lab., Mech. Engr. Dept., University of Washington, June 1963.
19. F. S. PRAMUK and J. W. WESTWATER, Effect of agitation on the critical temperature difference for a boiling liquid, *Chem. Engng Prog. Symp. Ser.*, no. 18, **52**, 79–83 (1956).
20. D. N. LYON, Peak nucleate-boiling heat fluxes and nucleate-boiling heat-transfer coefficients for liquid N_2, liquid O_2 and their mixtures in pool boiling at atmospheric pressure, *Int. J. Heat Mass Transfer* 7, 1097–1116 (1964).
21. R. SIEGEL and J. R. HOWELL, Critical heat flux for saturated pool boiling from horizontal and vertical wires reduced gravity, NASA Tech. Note TND-3123 (1965).
22. M. T. CICHELLI and C. F. BONILLA, Heat transfer to liquids boiling under pressure, *Trans. Am. Inst. Chem. Engrs* **41**, 755 (1945).
23. P. J. BERENSON, Transition boiling heat transfer from a horizontal surface, MIT Heat Transfer Laboratory Tech. Report no. 17 (1960).
24. J. H. LIENHARD and K. H. SUN, Effects of gravity and size upon film boiling from horizontal cylinders, *J. Heat Transfer* **92**, 292 (1970).
25. J. W. WESTWATER and J. G. SANTANGELO, Photographic study of boiling, *Ind. Engng Chem.* **47**, 1605 (1955).

LE FLUX DE CHALEUR MAXIMAL POUR L'ÉBULLITION EN RÉSERVOIR SUR DES CYLINDRES HORIZONTAUX

Résumé—Environ 440 observations originales du flux de chaleur maximal pour l'ébullition en réservoir dans une large gamme de tailles de gravités, de pressions réduites et de liquides en ébullition. Ces observations et un nombre égal de renseignements pour d'autres conditions obtenus à partir de la littérature sont corrélés avec une précision d'environ ± 20 pour cent en employant comme coordonnées le flux de chaleur sans dimensions en fonction du rayon sans dimension.

Une prévision analytique du flux de chaleur maximal est exposée. La prévision dépend en partie d'une "épaisseur de couche de vapeur". Des données supplémentaires forment la base d'une expression empirique

pour l'épaisseur de la couche. La substitution de ce résultat dans l'équation analytique fournit une équation générale précise pour le flux de chaleur maximal.

DER MAXIMALE WÄRMESTROM BEIM BEHÄLTERSIEDEN AN WAAGERECHTEN ZYLINDERN

Zusammenfassung—Etwa 440 eigene Messungen des maximalen Wärmestroms beim Behältersieden werden vorgelegt für einen weiten Bereich von geometrischen Grössen unterschiedlicher Gravitation, für verminderte Drücke und verschiedene Flüssigkeiten. Diese und eine gleiche Anzahl von Messwerten aus der Literatur für andere Bedingungen wurden korreliert und mit etwa ± 20 Prozent Abweichung ein dimensionsloser Wärmestrom über dem dimensionslosen Radius aufgetragen.

Eine analytische Gleichung für den maximalen Wärmestrom wurde entwickelt. Diese Beziehung hängt teilweise von einer "Dampfhüllendicke" ab. Zusätzliche Daten liefern die Basis für einen empirischen Ausdruck für die Deckschichtdicke. Durch Einsetzen dieses Ergebnisses in die analytische Gleichung ergibt sich eine genaue allgemeine Beziehung für die maximale Wärmestromdichte.

ПРЕДЕЛЬНЫЙ ТЕПЛОВОЙ ПОТОК ПРИ КИПЕНИИ В БОЛЬШОМ ОБЪЕМЕ НА ГОРИЗОНТАЛЬНЫХ ЦИЛИНДРАХ

Аннотация—Представлено примерно 440 непосредственных наблюдений по предельному тепловому потоку при кипении в большом объеме в широком диапазоне изменения размеров, плотности, давления и рода жидкостей. Данные этих опытов и аналогичные результаты, известные из литературы, обобщаются с точностью до 20% зависимостью между безразмерным тепловым потоком и безразмерными радиусом и координатами. Разработан аналитический метод расчета предельного теплового потока. Расчет в некоторой степени зависит от «толщины слоя пара». Дополнительные данные служат основой для электрического описания толщины слоя пара. Подстановка этого результата в аналитическое уравнение позволяет получить обобщенное уравнение для предельного теплового потока.